Solar influences on climate over the Atlantic / European sector

Lesley J. Gray, Will Ball, and Stergios Misios

Citation: AIP Conference Proceedings **1810**, 020002 (2017); doi: 10.1063/1.4975498
View online: http://dx.doi.org/10.1063/1.4975498
View Table of Contents: http://aip.scitation.org/toc/apc/1810/1
Published by the American Institute of Physics

Solar Influences on climate over the Atlantic / European Sector

Lesley J. Gray,[1,2, a)] Will Ball[3,4] and Stergios Misios[2]

[1]*National Centre for Atmospheric Science, U.K.*
[2]*Department of Physics, Oxford University, Clarendon Laboratory, Parks Road, Oxford, U.K.*
[3]*Institute for Atmospheric and Climate Science, Swiss Federal Institute of Technology Zurich, Universitaetstrasse 16, CHN, CH-8092 Zurich, Switzerland.*
[4] *Physikalisch-Meteorologisches Observatorium Davos World Radiation Centre, Dorfstrasse 33, 7260 Davos Dorf, Switzerland.*

[a)]Corresponding author: gray@atm.ox.ac.uk

Abstract. There is growing evidence that variability associated with the 11-year solar cycle has an impact at the Earth's surface and influences its weather and climate. Although the direct response to the Sun's variability is extremely small, a number of different mechanisms have been suggested that could amplify the signal, resulting in regional signals that are much larger than expected. In this paper the observed solar cycle signal at the Earth's surface is described, together with proposed mechanisms that involve modulation via the total incoming solar irradiance and via modulation of the ultra-violet part of the solar spectrum that influences ozone production in the stratosphere.

INTRODUCTION

There are several proposed mechanisms[1] through which the 11-year solar cycle (SC) could influence the Earth's climate, as summarised by Figure 1. These include: (a) the direct impact of solar irradiance variability on temperatures at the Earth's surface, characterised by variation in the total incoming solar irradiance (TSI); (b) the indirect impact of variations through the absorption of Ultra-Violet (UV) radiation in the upper stratosphere associated with the presence of ozone, with accompanying dynamical responses that extend the impact to the Earth's surface; (c) the indirect impact of variations in energetic particle fluxes into the thermosphere, mesosphere and upper stratosphere at high geomagnetic latitudes; and (d) the impact of variations in the generation of ions by galactic cosmic ray (GCR) penetration into the troposphere. Although different in their nature, these four pathways may not work in isolation but their influence could be synergetic. For example, there is modelling evidence that the influences of TSI at the surface in combination with the stratospheric response to the spectrally-resolved solar irradiance (SSI) variability could reinforce solar influences on regional scales, such as the tropical Pacific[2]. Furthermore, the surface imprint of energetic particle precipitation may be similar to influences of SSI variability[3].

This paper provides a summary of evidence and our current understanding of the first two of these proposed mechanisms, namely those involving solar irradiance variability, with a focus on surface impacts in the Pacific and in the Atlantic / European sector.

Radiation Processes in the Atmosphere and Ocean (IRS2016)
AIP Conf. Proc. 1810, 020002-1–020002-8; doi: 10.1063/1.4975498
Published by AIP Publishing. 978-0-7354-1478-5/$30.00

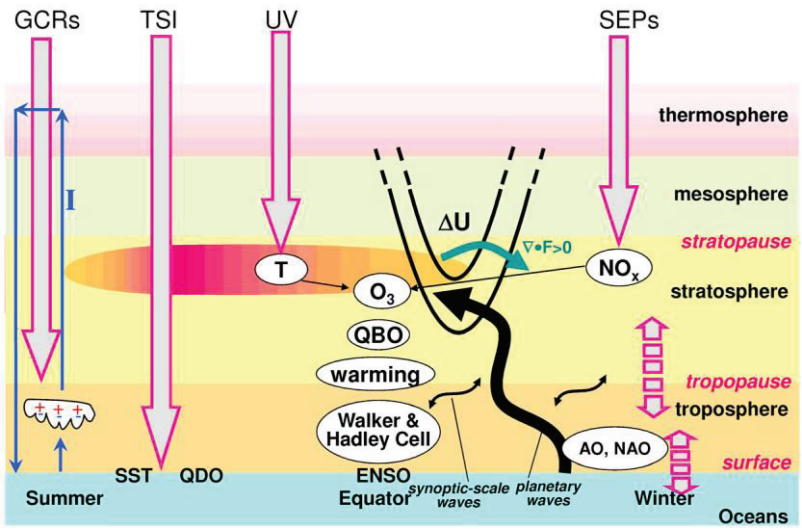

FIGURE 1. Schematic diagram of solar influence on climate showing direct and indirect effects of total solar irradiance (TSI), spectrally-resolved solar irradiance (SSI), energetic particles and galactic cosmic rays. Reproduced from L.J. Gray et al., Rev. Geophys. 48: RG4001, doi: 10.1029/2009RG000282 (2010), with the permission of Wiley Publishers.

SOLAR IRRADIANCE PROXIES

One of the primary challenges in this research field is the difficulty in identifying the optimal indicator of solar variability in the various wavelength bands. Direct satellite measurements of TSI, i.e. the total irradiance across all spectral bands, have been available since the late 1970s, starting with the NIMBUS7 Earth Radiation Budget (ERB) in 1978[4], and continuing to this day with the currently flying Solar Radiation and Climate Experiment (SORCE) Total Irradiance Monitor (TIM)[5] and TSI Continuity Transfer Experiment (TCTE)/TIM. However, this period encompasses less than four solar cycles, and is inadequate for the analysis of long-term data such as sea level pressure and temperature where global datasets extend back to the mid 19th century and for European datasets that extend even further back, to the 17th century. For these analyses a variety of 'proxy' data indices are employed to represent past solar variability, for example sunspot number. The situation is even more challenging for the analysis of responses that involve modulation of the amount of UV radiation, since direct observation of spectrally-resolved solar irradiance (SSI) over a wide range of UV wavelengths has only been achieved since 1981[6], and with sufficiently good stability to capture accurate solar cycle changes above 250 nm since 1991[7] with the Upper Atmosphere Research Satellite (UARS) Solar Ultraviolet Spectral Irradiance Monitor (SUSIM)[8]. There has also been much uncertainty in recent spectral observations from SORCE, particularly in the size of the change in UV radiation between solar minimum and solar maximum[9,10].

In order to provide a coherent best-estimate time-series of proxy indicators, the available observations are used alongside models of solar variability. There are currently two leading solar irradiance models that go back from present day to the 17th century and cover wavelengths from 115 nm to 100 microns or longer: the empirical NRLSSI-2 and the semi-empirical SATIRE model[11]. NRLSSI-2[12] is the latest version of the NRLSSI-1 model (used in the Coupled Model Inter-comparison Project, CMIP5); the update employs slight adjustments to its predecessor, but with the main change being to use SORCE UV data and SORCE/TIM TSI data to inform the reconstruction. Because of the high uncertainty (low stability) in spectral measurements on solar cycle timescales, NRLSSI-2 assumes that variability on solar rotational timescales (~27 days) can be scaled to the solar cycle, using the following steps: (i) removing short-term variability by subtracting the 81-day smoothed time series, (ii) regressing each detrended time series below 2,400 nm with a sunspot area proxy, to represent darkening, and the Mg II and F10.7 cm radio flux indices, to represent surface brightening, and then (iii) reproducing the full variability including the solar cycle by using the regression coefficients with the original brightening and darkening time series; above 2,400 nm models of the solar atmosphere are used to complete the spectrum. SATIRE, on the other hand, uses

model atmospheres to represent four time-independent irradiance components at all wavelengths: two for darkening, one for brightening, and a background for the time-invariant quiet Sun. Full-disk continuum intensity images and magnetograms are used to identify the distribution of dark and bright features on the surface, respectively, and by integrating the area coverage of each feature with respect to its distance from the disk centre, irradiance can be reconstructed. Prior to 1974 when full-disk images are not available, area coverage of each feature is estimated from a model that simulates magnetic flux transport based upon sunspot number, area and locations.

In terms of TSI, both models display a similar centennial-scale trend from 1883 to 1986, as can be seen in Fig. 2d; the trend during this period is in part defined by the sunspot number and areas, and therefore a similar source of information. After 1974, the two models have a different input to represent the bright and dark magnetic features, as described above, which is why the underlying trend (between minima) in the two models diverge. From 1986 to 2008, SATIRE-S displays a larger decline, reflecting the decline in surface total magnetic flux, while NRLSSI-2 remains essentially flat between minima, reflecting only very small changes between minima in the Mg II index used.

Spectral, inter-cycle trends largely reflect a similar tendency in each model, with respect to the TSI. In Fig 2a, the integrated flux between 176 and 242 nm in both models is largely similar, though after 1986, SATIRE exhibits a slightly larger solar cycle variability owing to the addition of the background, inter-cycle, decrease in irradiance. Above ~250 nm, the solar cycle variability in SATIRE increases with respect to NRLSSI-2 to being on average between 1.5 and 2 times larger than NRLSSI-2. This increase is clear in Fig. 2b, where the integrated region between 320 and 400 nm is shown, and while the difference is very much dependent on the cycle considered, the general picture is that SATIRE displays ~1.5 times larger variability over this region.

We note that the recommendation[13] for CMIP6 is for Climate Centres to use an average of the SATIRE and NRLSSI-2 values for the spectrally-resolved and total solar irradiances in their historical climate simulations (see also http://solarisheppa.geomar.de/cmip6).

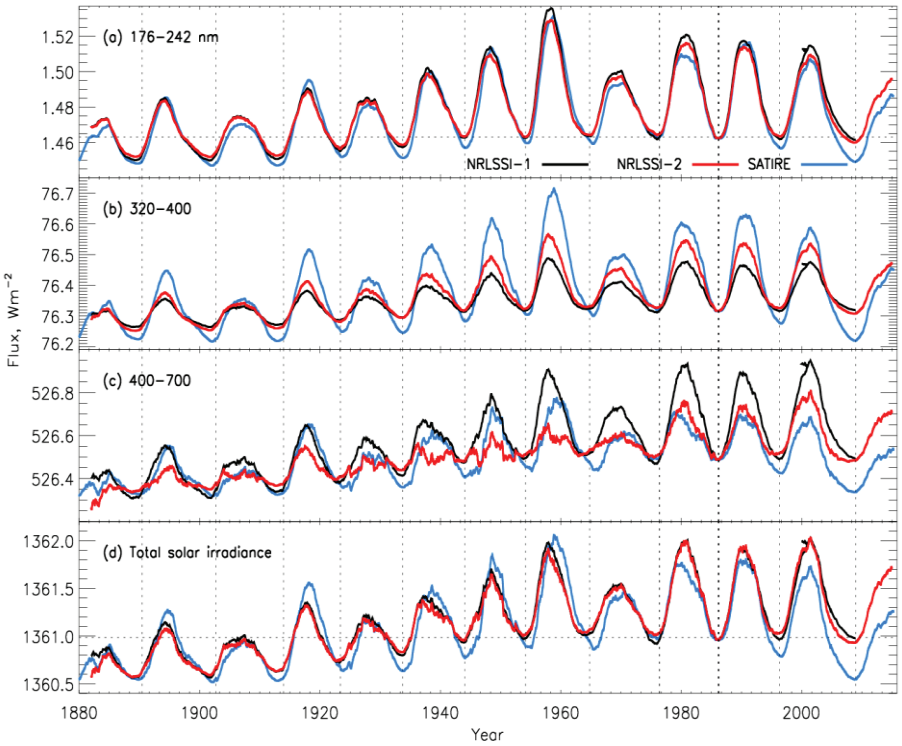

FIGURE 2. Solar irradiance variations from the SATIRE, NRLSSI-1, NRLSSI-2 models from 1880 to the present in four wavelength bands: (a) 176 - 242 nm (UV), (b) 320-400 nm (UV), (c) 400-700 nm (visible), and (d) TSI. The time series have been smoothed with a 13-month boxcar and NRLSSI-1 and -2 are shifted to match SATIRE in March 1986 (thick vertical dotted line). Vertical dotted lines indicate the start/end of cycles based on sunspot number.

THE GLOBAL MEAN SURFACE RESPONSE

Increased TSI at periods of solar maximum is expected to influence the Earth's surface directly, by enhancing the energy absorbed, provided that the global mean albedo remains unchanged (e.g. ice and cloud reflectance). This would lead to a modest positive temperature anomaly when averaged over the globe. Analysis of surface temperature observations show a 0.08 – 0.16 K global surface warming in solar maximum, depending on the dataset and methodology used[14,15]. The amplitude of this observed global surface warming is consistent with theoretical calculations assuming a solar heating of the upper global ocean (depth ~80-100m), and given the huge ocean heat capacity the response is likely to lag the solar forcing by 1-2 years[16]. Figure 3 (left panel) shows results from an analysis of historical simulations (1850-2005) performed as part of the CMIP5 activity and these indicate that the modelled surface response to the solar cycle is indeed characterized by a 1-2 year time lag[17]. Although there is large inter-model variability both in amplitude and timing, the multi-model ensemble mean (MMM) response is characterized by a positive temperature anomaly of about ~0.07 K at time lags of 1–2 years. The CMIP5 models, therefore, support the notion of a delayed global surface warming found in observation.

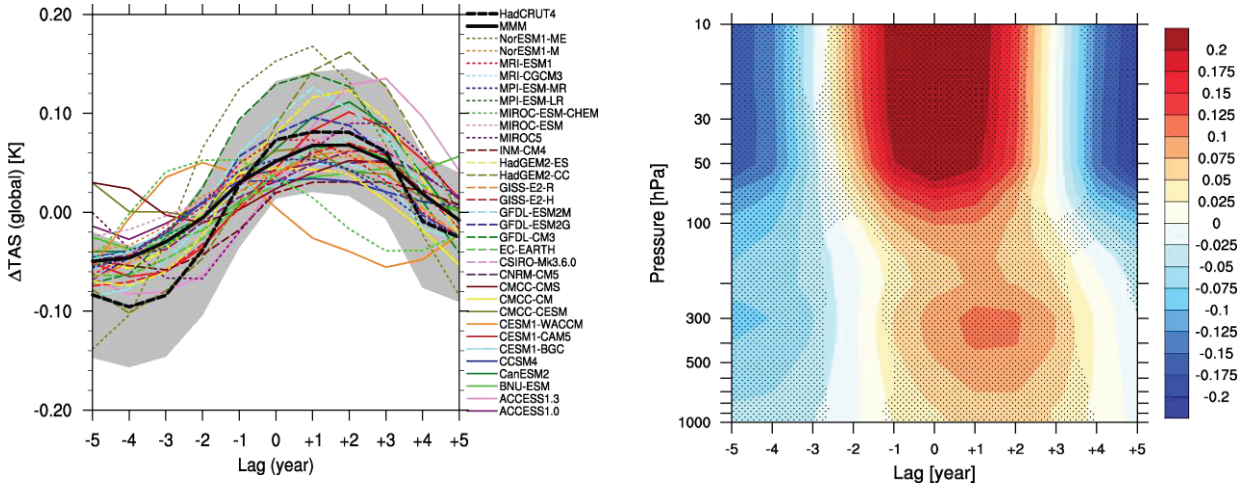

FIGURE 3. Left panel: Lagged solar regression coefficients of global mean air surface temperature for the CMIP5 historical simulations (1850-2005). Thick black solid line is the MMM response. HadCRUT4 temperature anomalies (thick black dashed line) and ±2σ range (grey shading) are shown for the 1950 – 2010 period. Reproduced from S. Misios et al., Q.J. Roy. Meteorol. Soc., 142:928-941, doi:10.1002/qj.2695 (2015), with the permission of Wiley Publishers. **Right panel:** Lagged solar regression coefficients of global mean air temperature for all CMIP5 models. Positive lags (in years) mean that the solar forcing leads the response. Units in K, assuming 1 Wm^{-2} TSI increase for a typical solar cycle. Reproduced from S. Misios et al., Q.J. Roy. Meteorol. Soc., 142:928-941, doi:10.1002/qj.2695 (2015), with the permission of Wiley Publishers.

The time-scale of the global mean warming (1–2 years) implies that the extra energy absorbed by the climate system in solar maxima is stored primarily in the upper layer of the ocean[16,18]. As with the global mean surface, there is model evidence that there is a time-delayed global troposphere warming. The CMIP5 models, for instance, suggest an upper tropospheric warming of 0.14 K at time lags +1 and +2 years after the solar maximum, which is almost twice the amplitude of the modelled surface warming (see Figure 3, right panel). The multi-model agreement in the CMIP5 models is high[17], although the amplitude of the tropospheric temperature anomalies differ markedly in some models. This delayed response suggests, at least in the global mean perspective, that SC signals in the troposphere are tightly linked to the delayed surface warming due to increased TSI. In contrast, the stratosphere warms roughly in phase with the SC forcing, as expected via the direct influence of the UV heating and the ozone feedback[19,20].

Clearly, the global mean surface warming in response to the SC is modest compared to effects of other external forcings. It is certainly much smaller than the radiative forcing associated with anthropogenic increases in GHG concentration. It is smaller even than the response to sporadic sulphate aerosol injection from major volcanic

eruptions that efficiently reflect the incoming shortwave radiation back to space, resulting in negative temperature anomalies lasting for the 1-3 following years e.g. after the eruption of Mt. Pinatubo in 1992. However, despite the very small global mean temperature response to SC forcing there is mounting evidence that *regional* signals associated with the SC can be much larger, due to the presence of positive feedbacks involving atmospheric wave-mean flow interactions and/or atmosphere-ocean coupling (e.g. Bjerknes feedback). In the following, we review proposed positive feedbacks that may amplify SC influences in the tropical Pacific and North Atlantic Ocean.

THE TROPICAL PACIFIC RESPONSE

Composite and regression analyses of surface temperature observations over the last century show a strong cooling in the East Pacific in peak years of solar maximum, with amplitude of about 1K at lag zero (Figure 4). Warmer water is found in the western sector extending off the coast of California, while in the North Pacific the dipole of negative/positive SST anomalies resembles the signature of the Pacific Decadal Oscillation. The negative SST response in the East Pacific peaks approximately 2 years before the peak of the 11 year solar cycle[21] and weakens in the years to follow (lags 1-3 years, Figure 4). Such a strong SC signal, can not be explained by direct radiative effects only and it has been suggested[22] that a positive dynamical / thermo-dynamical feedback could result in cold water in the tropical East Pacific. Increased surface ocean heating in solar maxima gives rise to enhanced evaporation, which converges by the prevailing easterlies into the convective precipitation zones, fuelling extra energy when it condenses to form rain. This additional latent heat energy stimulates the large zonal overturning (Walker) circulation in the Equatorial Pacific. As a result, the surface easterlies strengthen and more cold water is upwelled in the tropical East Pacific, thus explaining the observed cooling in that region at solar maximum. Amplified subsidence in the tropical East Pacific also reduces cloud cover, allowing stronger surface heating, thus completing the positive feedback loop. This dynamical / thermo-dynamical mechanism is present in some climate models but it is found weak in the majority of the CMIP5 models. Instead, temperatures in the equatorial Pacific show a weak surface warming at all longitudes, lagging the solar cycle by 1-2 years[17]. It is not clear whether this means that the models are deficient in reproducing this feedback response, or whether the direct effect of increased TSI is indeed a warmer Pacific[16] and the observational record is insufficiently long for the signal to be accurately diagnosed[23].

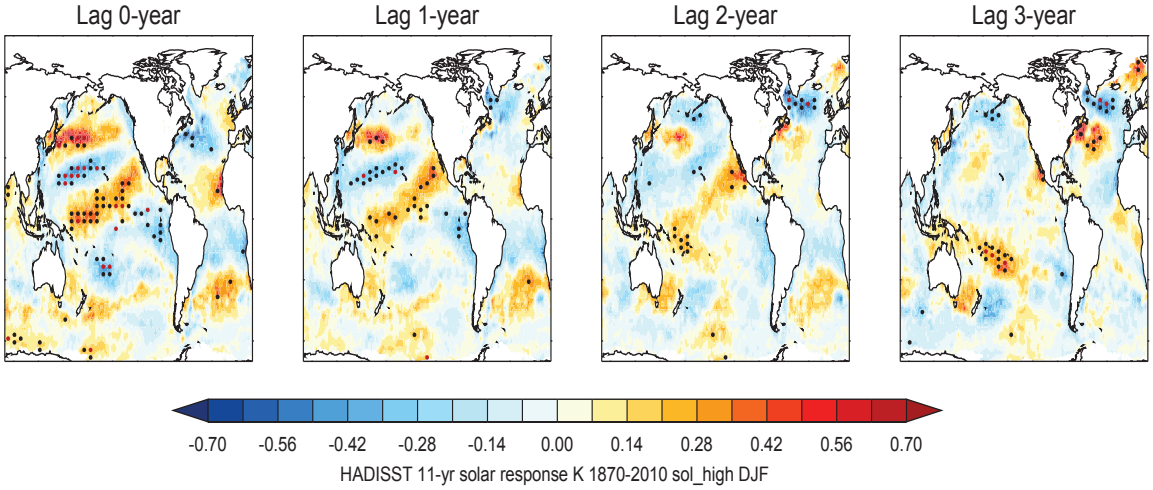

FIGURE 4. Regression analysis of the winter-time (DJF) sea surface temperatures (HadISST 1870-2010) associated with the solar cycle over different time lags (in years). A positive lag indicates that the solar forcing leads the response. Black (red) dots indicate statistical significance at the 95% (99%) level using a 2-sided Students' t-test.

THE NORTH ATLANTIC RESPONSE

Besides the SC signals in the tropics, analyses of the past few decades have suggested a SC signal in the Northern Hemisphere (NH) high latitudes. For example, a SC signal was suggested[24] in the winter North Atlantic Oscillation (NAO), a measure of surface pressure anomalies between the Icelandic Low and Azores High, the strength of which significantly influences European weather conditions. Further studies have suggested a SC signal in the duration and/or frequency of the occurrence of blocking events over the Atlantic in winter, in which a region of high pressure remains stationary for long periods, and this can also substantially affect European weather[25,26]. However, analyses that extend further back in time are less convincing. For example, the regression analysis by Roy and Haigh (2010)[23] also examined the SC in mean sea level pressure using the HadSLP dataset for the period 1870-2010 and found no statistically significant response in the Atlantic region.

However, if the regression analysis is repeated with the mslp lagging the solar index[27], as shown in figure 5, a clear signal emerges at 3-4 years that is statistically significant at the 99% level using a (2-sided) Students t-test. A positive pressure anomaly of up to 3 hPa difference between Smax/Smin is evident over the Azores region. This pattern of SC mslp response, and the corresponding sea surface temperature response (not shown, but see figure 5 of Gray et al. 2013) is consistent with a positive NAO anomaly approximately a quarter cycle (3-4 years) following solar maximum. This does not, however, produce a statistically significant signal in the NAO index itself (remember that the NAO is a measure of the *difference between anomalies* over the Azores and Iceland) since any SC response in the Icelandic region, where the background variability is much higher, is not sufficiently strong to clearly emerge from the background variability.

This lagged response in mslp over the Azores remains significant even when the regression analysis is extended back in time to 1660[28] using a reconstructed dataset over the European / Atlantic sector. This adds further support for the presence of an amplified SC response over the Atlantic region and thus the potential for improved European seasonal and decadal weather forecasts.

A potential influence route for this enhanced SC impact over the Atlantic has been suggested[29,30], via the so-called 'top-down' influence, associated with increased ozone production / heating[31] in the upper equatorial stratosphere at solar maximum. Positive (negative) temperature anomalies at Smax (Smin) in the equatorial upper stratosphere are accompanied by anomalous westerlies (easterlies) in the subtropics, through the requirement to maintain thermal wind balance. This in turn is thought to be a major influence on the propagation of planetary waves in winter. A mechanistic stratosphere-mesosphere model study has shown[32] that a relatively small easterly perturbation imposed in the NH subtropical upper stratosphere in early winter had a profound effect on the direction of wave propagation and hence on the development of sudden stratospheric warmings (SSWs), such that SSWs occurred more predictably and much earlier than in the corresponding control ensemble that had no additional easterly forcing. If this mechanism operates in the atmosphere then, on average, one would expect a warmer, more disturbed polar vortex with more frequent SSWs in Smin years than in Smax years. This influence is captured in some climate models[33,34,35]. However, observational data for the stratosphere are only available since the ~1950s and analysis of the impact of the SC on the polar vortex is further complicated by the influence of the quasi biennial oscillation (QBO) in the lower stratosphere[36] which also influences wave propagation and hence the polar vortex[37].

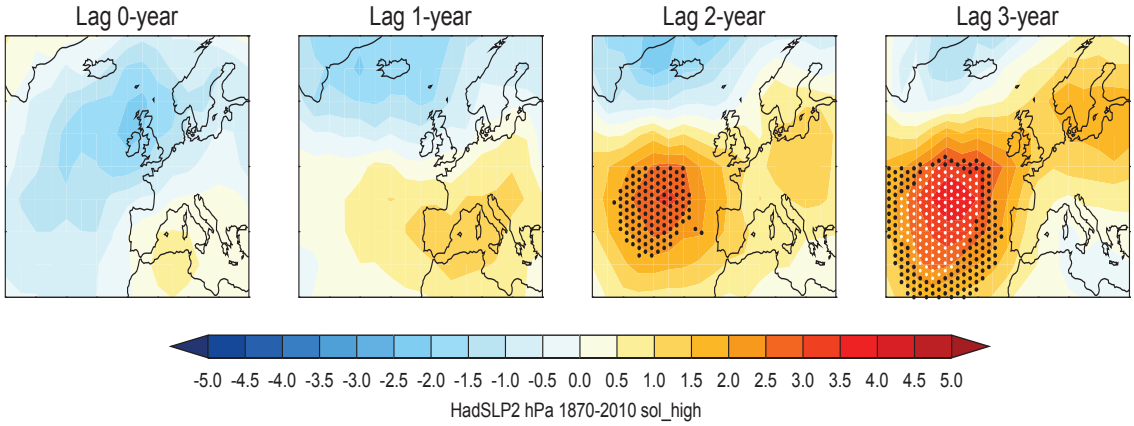

FIGURE 5. Regression analysis of the winter-time (DJF) sea level pressure (Hadslp 1870-2010) associated with the solar cycle over different time lags (in years). A positive lag indicates that the solar forcing is leading. Black (white) dots indicate statistical significance at the 95% (99%) level using a 2-sided Students' t-test.

The stratospheric polar vortex is a deep structure that extends throughout the depth of the winter polar stratosphere (10-50km), so the above mechanism can explain the penetration of the SC influence from the equatorial upper stratosphere deep into the lower stratosphere polar region in winter. Numerous studies over recent years[38,39] have demonstrated that the zonal winds in the lower stratosphere in winter can influence the evolution of the underlying troposphere, and in particular the position of the mid-latitude Atlantic jetstream. This provides a mechanism for the SC influence to extend to the surface, since positive NAO anomalies have been associated with periods of a strong, undisturbed polar vortex and negative NAO anomalies are frequently observed to follow a SSW, when the polar vortex is severely disrupted.

The forcing of an NAO anomaly in this way can, in turn, influence the sea surface temperature (SST) of the Atlantic, resulting in a well-known tri-polar distribution. This SST response to NAO-forcing has been invoked as a possible mechanism to explain the 3-4 yr (~quarter solar cycle) lag of the mslp response over the Atlantic (Scaife et al. 2013). Because the depth of the ocean mixed layer displays a strong seasonal cycle, any SST anomaly produced during the winter (as a result of an NAO anomaly) is likely to persist below the mixed-layer during the following summer and evidence has been found for its re-emergence at the beginning of the following winter. This therefore presents the possibility of a positive feedback on the NAO anomaly via the ocean. For example, during periods of solar maximum, the atmospheric (top-down) SC forcing of a positive NAO anomaly can be enhanced by additional forcing of a positive NAO through feedback via the ocean from the previous winter's SST anomaly. This reinforced response via the ocean would enhance the NAO anomaly year-on-year until the top-down SC forcing switched from Smax to Smin, thus resulting in a surface response that lags the SC forcing by one quarter of a cycle.

There is some evidence that models are able to capture this feedback mechanism via the Atlantic Ocean SST response (Andrews et al. 2015) but the simulated response is much smaller than the observations suggest. Closer examination of surface observations has also provided supporting evidence of this proposed feedback mechanism. In a regression analysis of the individual winter months[28] it was found that the maximum mslp SC response in late winter (February) was at lag-zero i.e. concurrent with the SC forcing, consistent with the immediate forcing of the NAO via the stratospheric polar vortex (note that SSWs are more prevalent in late winter). On the other hand, the maximum mslp SC response in early winter (December) was found at lags of ~3-4 years, consistent with the positive feedback mechanism through re-emergence of the SST signal. When averaged over the whole winter (December-January-February) the signals averaged out to give a maximum signal at lags of ~3 years. It is important to note that this proposed amplification mechanism relies on the presence of NAO anomalies of the same sign in successive winters. In reality, the polar vortex and the NAO are influenced by many other factors e.g. the QBO and ENSO that can disrupt this sequence of successive NAO same-signed anomalies, and thus disrupt the positive feedback process that causes the lagged response in early winter. Because of this, it is possible that the analysed lag of the maximum

DJF SC response will depend on the time-interval examined, varying from ~3 years when the feedback mechanism is un-interrupted, to zero-lag when the feedback process is substantially disrupted by another influence. This raises difficulties for the unambiguous identification of a SC signal in the NAO and could explain the fact that although the maximum SC signal in mslp is found at ~3 years when the whole data period 1870-2010 is employed, analysis of the more recent past (e.g. since 1979 when good satellite data are available) shows the peak response at lags of 0-2 years.

REFERENCES

1. L. J. Gray et al., Rev. Geophys. **48**: RG4001, doi: 10.1029/2009RG000282 (2010).
2. G. A. Meehl et al., Science, **325** (5944): 1114-1118,(2009).
3. E. Rozanov et al., Surv. Geophys., **33**(3-4): 483-501 (2012).
4. G.A. Chapman et al., J. Geophys. Res., **101**, 13541–13548 (1996).
5. G. Kopp et al.. Sol. Phys., **230** (1), 129–140, doi: 10.1007/s11207-005-7433-9 (2005).
6. G. J. Rottman, et al., Geophys. Res. Lett., **9**, 587–590, doi: 10.1029/GL009i005p00587 (1982).
7. K. L. Yeo, et al., JGR-Space Physics, **120,** doi: 10.1002/2015JA021277 (2015).
8. L. E. Floyd et al., Adv. Space Res., **31**, 2111–2120, doi:10.1016/ S0273-1177(03)00148-0 (2003).
9. W. T. Ball, et al., J. Atmos. Sci., **71,** 4086-4101. doi: 10.1175/JAS-D-13-0241.1 (2014).
10. M. Scholl et al., Space Weather Space lim., 6, A14, doi: 10.1051/swsc/2016007 (2016).
11. N. A. Krivova et al., J. Geophys. Res., **115,** A12112, doi: 10.1029/2010JA015431 (2010).
12. O. Coddington, et al., BAMS, **97,** 1265, 2016, BAMS-D-14-00265.1 (2016).
13. K. Matthes et al., Solar Forcing for CMIP6 (v3.1). Geosci. Model Dev. Discuss., 1-82 (2016).
14. D. H. Douglass and B. D. Clader, Geophys. Res. Lett., **29 (**16): 1786 (2002).
15. K. K. Tung and C. D. Camp, J Geophys Res-Atmos, **113** (D5): D05114 (2008).
16. W. White et al., J Geophys Res-Oceans, **102** (C2), 3255-3266 (1997).
17. S. Misios et al.,. Q. J. Roy. Meteorol. Soc.. 142: 928 – 941, doi:10.1002/qj.2695 (2015).
18. M. B. Andrews et al., Environ. Res. Lett. **10**, 054022, doi: 10.1088/1748-9326/10/5/054022 (2015).
19. J. D. Haigh, Science **272**: 981–984, doi: 10.1026/science.272.5264.981 (1996).
20. L. J. Gray, et al., (2009), J. Atmos. Sci., **66**, 2402–2417, doi:10.1175/2009JAS2866.1 (2009).
21. L. J. Gray et al., J. Geophys. Res. **118**, 13405–13420, doi: 10.1002/2013JD020062 (2013).
22. G. A. Meehl, et al., J. Clim., **21**(12), 2883-2897 (2008).
23. I. Roy and J. D. Haigh, Atmos. Chem. Phys., **100,** 3147–3153 (2010).
24. K. Kodera, (2002), Geophys. Res. Lett., **29**(8), 1218, doi:10.1029/2001GL014557 (2002).
25. D. Barriopedro et al., J. Geophys. Res. **113**, D14118, doi: 10.1029/2008JD009789 (2008).
26. T. Woollings et al., Geophys. Res. Lett. **37**, L20805, doi: 10.1029/2010GL044601 (2010).
27. L. J. Gray, L.J. et al., J. Geophys. Res. **118**, 13,405–13,420, doi: 10.1002/2013JD020062 (2013).
28. L. J. Gray, et al., Q. J. R. Meteorol. Soc. **142**, 1890 – 1903, July 2016 A DOI:10.1002/qj.2782 (2016).
29. K. Kodera and Y. Kuroda, J. Geophys. Res., **107** (D24), 4749, doi:10.1029/2002JD002224 (2002).
30. Y. Kuroda and K. Kodera, J. Meteorol. Soc. Jpn., **80** (4B), 973-984 (2002).
31. J. D. Haigh, Phil. Trans. R. Soc. London, Ser. A, **361**, 95–111, doi:10.1098/rsta.2002.1111 (2003).
32. L. J. Gray, et al., J. Atmos. Sci., **61**, 2777–2796, doi:10.1175/ JAS-3297.1 (2004).
33. K. Matthes, et al., J Geophys Res-Atmos, **109** (D6), D06101 (2004).
34. S. Ineson et al., Nat. Geosci. **4**: 753–757, doi: 10.1038/ngeo1282 (2011).
35. D. M. Mitchell et al., Q. J. R. Meteorol. Soc. **141**, 2011–2031, doi: 10.1002/qj.2492 (2015).
36. K. Labitzke and H. van Loon J. Atmos. Terr. Phys., **50**, 197–206 (1988).
37. J. R. Holton and H.-C. Tan, J. Meteorol. Soc. Jpn., **60,** 140–148 (1982).
38. M. P. Baldwin and T. J. Dunkerton, Science, **294,** 581–584, doi:10.1126/science.1063315 (2001).
39. J. Kidston et al., Nat. Geosci. **8**, 433 – 440, doi: 10.1038/ngeo2424 (2015).